Calculation of Phenomenological Nucleon-Nucleon Potentials*

J. L. GAMMEL, R. S. CHRISTIAN, AND R. M. THALER
Los Alamos Scientific Laboratory, Los Alamos, New Mexico
(Received August 27, 1956)

An attempt to find a phenomenological nucleon-nucleon potential is described. The class of charge and velocity independent potentials with central and tensor parts of Yukawa shape with a hard core is considered. The depths, ranges, and core radii of such potentials with general spin and parity dependence are adjusted to fit experimental data. No potential of this type is found which fits all of the data.

I. INTRODUCTION

A LARGE amount of new experimental data[1] on nucleon-nucleon scattering has become available recently. These new data and the availability of high-speed computing machinery make possible a more complete examination of the classic problem of finding a charge- and velocity-independent phenomenological nucleon-nucleon potential.

The experimental data referred to in the following are the data on the bound state of the deuteron and the nucleon-nucleon scattering data in the energy range $E_{\text{lab}} \leq 340$ Mev.

A specific shape is assumed for the potentials. A systematic procedure for fitting certain data is presented. This procedure uniquely determines the parameters which characterize the potentials.

The potentials so determined do not fit all of the experimental data. However, it is anticipated that these potentials will serve as a reasonable starting point for other calculations. For example, the even-parity potentials found in this work have already proved useful in the calculation of some properties of heavy nuclei using the method of Brueckner.[2]

Feshbach and Schwinger[3] have examined the effect of a tensor force in the two-nucleon problem. They considered the bound state of the deuteron and the low-energy triplet scattering in order to determine the parameters which characterize the triplet even-parity potential. In their work, they assumed a potential of Yukawa shape without a core. The present investigation extends this work to higher energies for both n-p and p-p scattering in order to determine the parameters characterizing the other parts of the potential. However, previous work[4] seems to indicate that potentials of this form are not adequate to fit the data; in particular, it appears that the high-energy p-p data suggest the presence of a repulsive core in the interaction.[5] The high-energy n-p total cross sections are likewise most readily explained by the inclusion of a repulsive core. Meson theories likewise indicate such cores.[6]

For these reasons the work in this paper has been carried out with potentials of the Yukawa shape as used by Feshbach and Schwinger with the addition of a hard core.[7]

This choice of a specific shape is a serious limitation. Neglect of possible spin orbit terms in the potential may also be a serious limitation.

II. FORM OF THE POTENTIALS

The potentials considered in this paper are all of the form

$$\begin{aligned} &V(r)=\infty, && r<r_0 \\ &V(r)=V_c(r)+V_t(r)S_{12}, && r>r_0, \end{aligned} \tag{1}$$

where S_{12} is the tensor operator.[8] The potentials are assumed to have a Yukawa shape; that is,

$$\begin{aligned} &V_c(r)=-V_c\exp(-r/r_c)/(r/r_c), \\ &V_t(r)=-V_t\exp(-r/r_t)/(r/r_t), \\ &\mu_c\equiv 1/r_c, \quad \mu_t\equiv 1/r_t. \end{aligned} \tag{2}$$

The five parameters V_c, r_c, V_t, r_t, and r_0 depend on the spin and parity ($V_t=0$ for $S=0$). We assume that the radius of the hard core is independent of parity, but not necessarily the spin. The reason for this assumption is that the odd-parity scattering does not depend sensitively on the radius of a small hard core unless the potential is very singular. Thus the calculation depends on fourteen parameters.

These are systematically determined by requiring that the potentials fit certain experimental quantities exactly. There are two bases for the choice of these experimental quantities.

* Work performed under the auspices of the U. S. Atomic Energy Commission.

[1] For summaries of nucleon-nucleon scattering data, see for example, Wilmot N. Hess, University of California Radiation Laboratory UCRL-4639, 1956 (unpublished). Stapp, Ypsilantis, and Metropolis, preceding paper [Phys. Rev. **105**, 302 (1957)] have a summary of the recent Berkeley polarization experiments at 310 Mev. Other polarization data are summarized in a review by D. Feldman, *Proceedings of the Sixth Annual Rochester Conference on High Energy Nuclear Physics* (Interscience Publishers, Inc., New York, 1956). An expanded version of this review will be published by Feldman.

[2] K. Brueckner (private communication).

[3] H. Feshbach and J. Schwinger, Phys. Rev. **84**, 194 (1951).

[4] R. S. Christian, Repts. Progr. in Phys. **15**, 68 (1952).

[5] R. Jastrow, Phys. Rev. **81**, 165 (1951).

[6] Maurice M. Lèvy, Phys. Rev. **84**, 441 (1951); Solomon Gartenhaus, Phys. Rev. **100**, 900 (1955); K. Brueckner and K. Watson, Phys. Rev. **92**, 1023 (1953); M. Taketani, Progr. Theoret. Phys. (Japan) **7**, 35 (1952).

[7] The inclusion of a hard core means that the potential is taken to be infinite and repulsive for distances less than the core radius.

[8] J. Ashkin and Ta-You Wu, Phys. Rev. **73**, 973 (1948).

TABLE I. Triplet even-parity potentials which fit the binding energy of the deuteron, the quadrupole moment of the deuteron, and the zero-energy n-p triplet scattering length.

Identification number	${}^3r_0$ (10^{-13} cm)	${}^3r_t{}^+/{}^3r_c{}^+$	${}^3V_c{}^+$ (Mev)	${}^3r_c{}^+$ (10^{-13} cm)	${}^3V_t{}^+$ (Mev)	${}^3r_t{}^+$ (10^{-13} cm)	$\%D$
15	0	1.022	28.28	1.460	33.81	1.493	3.57
16		1.922	61.69	1.111	12.28	2.135	2.55
12	0.1	1.022	37.07	1.216	62.00	1.244	4.55
13		1.922	115.4	0.8696	24.90	1.671	3.41
14		2.857	146.8	0.8475	8.982	2.421	2.34
9	0.2	1.022	47.74	1.039	105.0	1.062	5.40
10		1.922	198.0	0.7407	39.72	1.424	3.98
11		2.857	278.2	0.7067	14.31	2.019	2.78
1	0.3	1.022	65.10	0.9217	162.0	0.9423	6.05
2		1.922	338.5	0.6494	59.8	1.248	4.50
3		2.857	595.7	0.5714	26.0	1.633	3.45
4	0.4	1.022	100.7	0.8130	257.0	0.8312	6.56
5		1.922	659.3	0.5405	110.6	1.039	5.32
6		2.857	1308	0.4762	44.79	1.361	4.10
7		4.0	2640	0.3921	30.00	1.568	3.77
8	0.5	4.0	6395	0.3405	45	1.362	4.19

Some (such as the binding energy of the deuteron) are known so well experimentally that it seems unnecessary to consider the effect of fitting a slightly different value.

Some are chosen to keep the discussion systematic and within bounds. For example, we have chosen to require that our potentials fit the value of the p-p differential cross section at 90° in the center-of-mass system as a function of energy. This quantity is not known with so great precision as the binding energy of the deuteron. Nevertheless, we have settled on some values and fit them exactly.

The accurately known data come from low-energy experiments ($E_{\text{lab}} \leq 20$ Mev) and thus help determine the potentials for even-parity states. Choices of the second kind are made from high-energy data (90 Mev and over).

III. LOW-ENERGY DATA AND THE EVEN-PARITY POTENTIALS

A. The Triplet Even-Parity Potential

This is the potential for the ground state of the deuteron. The potential is adjusted to fit

TABLE II. Singlet even-parity potentials which fit the zero energy n-p and p-p scattering length and effective range.

${}^1r_0$ (10^{-13} cm)	${}^1\mu_c{}^+$ (10^{13} cm^{-1})	${}^1V_c{}^+(n\text{-}p)$ (Mev)	${}^1V_c{}^+(p\text{-}p)$ (Mev)
0.1	0.97	78.90	77.24
0.2	1.1	131.7	128.8
0.3	1.26	232.5	227.4
0.4	1.45	434.8	425.5
0.5	1.7	914.6	896.6
0.6	2.0	2117	2078
0.8	3.0	23 590	23 207
0.9	3.28	···	55 317

(1) the binding energy of the deuteron (2.228 Mev).

(2) the electric quadrupole moment of the deuteron (2.74×10^{-27} cm^2).

Recent calculations[9] suggest that field-theory corrections to this quantity are not important.

The percent D state is calculated but not used to reduce the number of parameters. It lies within the limits 2–7% for all potentials that we have considered. A recent evaluation[10] of various contributions to the magnetic moment of the deuteron gives $(3\pm1)\%$ for the percent D state. An upper bound of 4% for the percent D state requires the same thing in terms of potentials as other limits we find in the problem (see Fig. 4) and so agrees with them.

(3) The ${}^3S$ n-p scattering length (5.38×10^{-13} cm).

These experimental quantities reduce the number of parameters required to describe the triplet even-parity potential to two. These were taken to be ${}^3r_0$ and ${}^3r_t{}^+/{}^3r_c{}^+$.

A table of triplet even-parity potentials satisfying these conditions is shown in Table I.

B. The Singlet Even-Parity Potential

Since there is no tensor force in the singlet potentials, only three parameters are needed to describe the singlet even-parity potential. This number is reduced to one by the following conditions:

(4) The ${}^1S$ n-p scattering length is 23.68×10^{-13} cm.

(5) The ${}^1S$ n-p and p-p effective range is 2.7×10^{-13} cm.

We have calculated both the p-p and n-p effective range, and have not found a potential for which they are not equal (taking into account the slight difference in depth of n-p and p-p potentials due to electromagnetic effects; see immediately below). Thus the assumption that the n-p ${}^1S$ effective range, which is not known with great accuracy from the low-energy total cross section measurements, is the same as the more precisely known p-p ${}^1S$ effective range appears justified.

We have taken the p-p scattering length to be 7.66×10^{-13} cm.[11] A potential which makes the singlet n-p scattering length 23.68×10^{-13} cm will not make the p-p scattering length 7.66×10^{-13} cm. Presumably, the p-p potential has to be slightly less deep; the difference is presumed to be due to electromagnetic effects.[12] In calculating p-p angular distributions, we have used the p-p depths; in calculating n-p angular distributions, the n-p depths.

[9] J. Bernstein and A. Klein, Phys. Rev **99**, 966 (1955)

[10] M Suguwara, Phys. Rev. **99**, 1601 (1955).

[11] J. Jackson and J. Blatt, Revs. Modern Phys. **22**, 77 (1950). This is the value for small singlet shape-dependent parameter. Yukawa potentials with hard cores give small shape-dependent parameters.

[12] Julian Schwinger, Phys. Rev. **78**, 135 (1950). This has not been proved when a core is present in the potential.

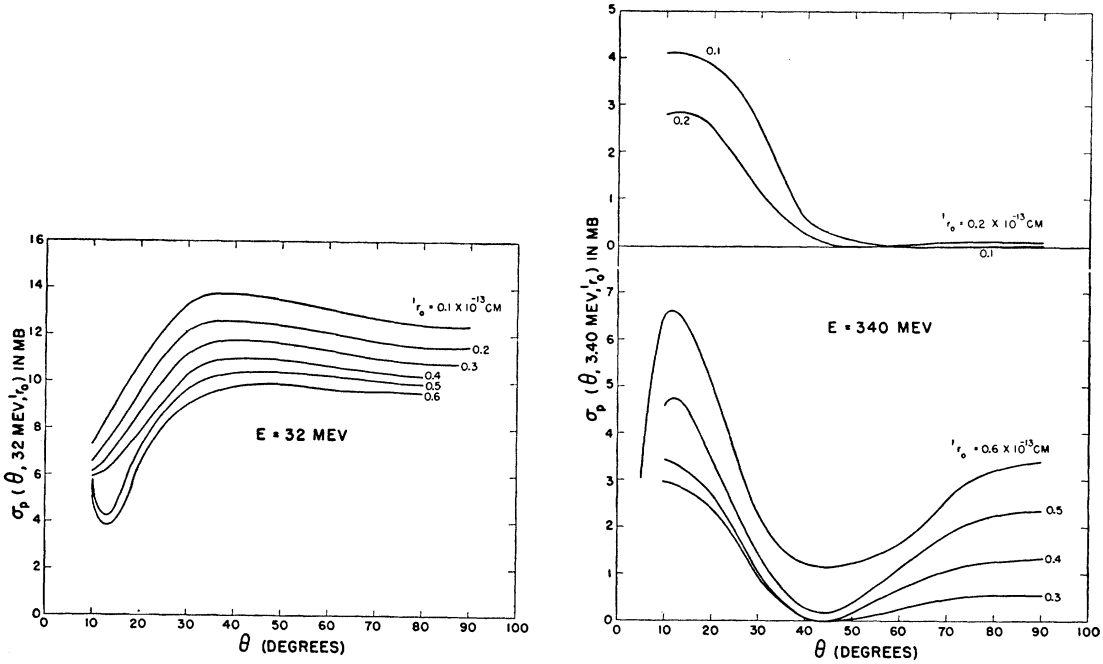

FIG. 1. ${}^1\sigma_p(\theta,E,{}^1r_0)$ *vs* θ for $E=32$ and 340 Mev and the singlet even-parity potentials of Table II.

We chose ${}^1r_0$ to be the parameter describing the singlet even-parity potential. A table of singlet even-parity potentials satisfying these conditions is shown in Table II.

IV. HIGH-ENERGY *p-p* DATA

The first high-energy data we consider is the *p-p* differential cross section at 90° in the center-of-mass system as a function of energy. We call this quantity $\sigma_p(90°,E)$.

In the following, ${}^1\sigma_p(90°,E;{}^1r_0)$ is the contribution of the singlet even-parity potential whose core size is ${}^1r_0$ (these potentials are given in Table II) to $\sigma_p(90°,E)$. The difference between our adopted experimental values of $\sigma_p(90°,E)$ and ${}^1\sigma_p(90°,E;{}^1r_0)$ is given in Table III.[13]

Plots of ${}^1\sigma_p(\theta,E;{}^1r_0)$ for $E=32$ and 340 Mev are shown in Fig. 1.

Let ${}^3\sigma_p(90°,E;{}^3r_0)$ be the contribution of the triplet odd-parity potential to $\sigma_p(90°,E)$. It is necessary to find some triplet odd-parity potential for which

$$ {}^3\sigma_p(90°,E;{}^3r_0)=\sigma_p(90°,E)-{}^1\sigma_p(90°,E;{}^1r_0). \quad (3) $$

We shall show that this can be done only for ${}^1r_0=0.5\times10^{-13}$ cm.

The reason for choosing to fit $\sigma_p(90°,E)$ as a function of energy is the following. ${}^3\sigma_p(90°,340\text{ Mev};{}^3r_0)$ is independent (approximately) of the central part of the triplet odd-parity potential.[14] Thus, adjusting the triplet odd-parity tensor potential in such a way that Eq. (3) is satisfied for $E=340$ Mev determines ${}^3V_t^-$ as a function of ${}^3\mu_t^-$. This function obviously depends on ${}^1r_0$ which appears on the right hand side of Eq. (3). It also depends on ${}^3r_0$ but not sensitively, because a small hard core has little effect in odd parity states.

We assume that ${}^3V_t^-$ is negative. The reason for this is the following. The minimum in $\sigma_n(\theta,E)$ (the *n-p* differential cross section at energy E) occurs at $\theta=80°$ for $E=90$ Mev. A potential with no odd-parity part (a Serber potential) puts the minimum in $\sigma_n(\theta,E)$ at $\theta=90°$ for all energies. Adding a negative ${}^3V_t^-$ to a Serber potential shifts the minimum towards 80°; a

TABLE III. The difference between the experimental values of $\sigma_p(90°,E)$ and ${}^1\sigma_p(90°,E;{}^1r_0)$ for various energies and singlet core sizes.

${}^1r_0$ (10^{-13} cm)	$\sigma_p(90°,E)-{}^1\sigma_p(90°,E;{}^1r_0)$ in mb					
	18.3	32	95	147	240	340 Mev
0.1	0.60	1.90	3.00	3.17	3.60	3.54
0.2	1.56	2.81	3.50	3.60	3.69	3.74
0.3	2.23	3.48	4.00	3.72	3.44	3.14
0.4	2.80	4.06	4.20	3.58	2.79	2.49
0.5	3.11	4.42	4.30	3.38	1.80	1.40
0.6	3.55	4.82	4.42	2.64	0.50	0.30

[13] This difference must be positive. For core sizes ${}^1r_0>0.5\times10^{-13}$ cm, this difference is negative for $E=340$ Mev and such core sizes must be ruled out. ${}^1\sigma_p(\theta,E;{}^1r_0)$ for any θ must be less than the experimental value. When we look at $\theta=30°$ we see that ${}^1r_0=0.1\times10^{-13}$ cm is ruled out by the 32-Mev *p-p* data. In order to keep $\sigma_p(\theta,340$ Mev) flat down to $\theta<10°$, it would be best to choose ${}^1r_0=0.2$ or 0.3×10^{-13} cm. Plots of ${}^1\sigma_p(\theta,E;{}^1r_0)$ for $E=32$ and 340 Mev are shown in Fig. 1. From such arguments, it appears that $0.2<{}^1r_0<0.5\times10^{-13}$ cm, independently of what is assumed about the triplet odd-parity states.

[14] In Born approximation (for which the scattering amplitudes are strictly linear in the potentials), ${}^3\sigma_p(90°,E;{}^3r_0)$ is independent of ${}^3V_c^-$ at any energy.

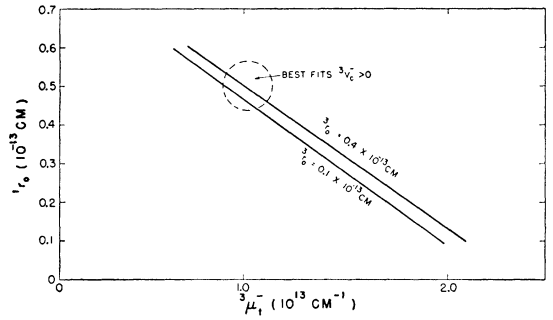

FIG. 2. $^3\mu_t^-$ *vs* $^1r_0$ for various $^3r_0$. The straight lines are obtained by satisfying Eq. (3) for $E=32$ and 340 Mev with triplet odd-parity potentials having no central part.

positive $^3V_t^-$ shifts the minimum toward 100°. Also, a negative $^3V_t^-$ is in agreement with potentials calculated from meson theory.[6]

If $^3V_c^-=0$, and if Eq. (3) is also satisfied for $E=32$ Mev, only one value of $^3\mu_t^-$ is possible for each $^3r_0$ and $^1r_0$. Figure 2 shows these values of $^3\mu_t^-$ as a function of $^1r_0$ for various $^3r_0$. Table IV shows triplet odd-parity potentials having no central part which satisfy Eq. (3) for $E=32$ and 340 Mev.

When $^3V_c^-$ is not zero, it is possible to use other values of $^3\mu_t^-$ than the ones read from Fig. 2. For given $^1r_0$, $^3\mu_t^-$ [which determine the value of $^3V_t^-$ since Eq. (3) must be satisfied at $E=340$ Mev] and several values of $^3\mu_c^-$, we determine $^3V_c^-$ so that Eq. (3) is satisfied for $E=32$ Mev.

We find that it is not possible to get far away from the curve in Fig. 2. The reason for this is that $^3V_c^-$ increases away from the curve, and $^3\sigma_p(40°,32\text{ Mev};^3r_0)$ increases much more rapidly than $^3\sigma_p(90°,32\text{ Mev};^3r_0)$ with increasing $^3V_c^-$. With even a small $^3V_c^-$ the angular distribution at $E=32$ Mev will not fit the experimental angular distribution for any $^1r_0$. This is illustrated in Fig. 3.

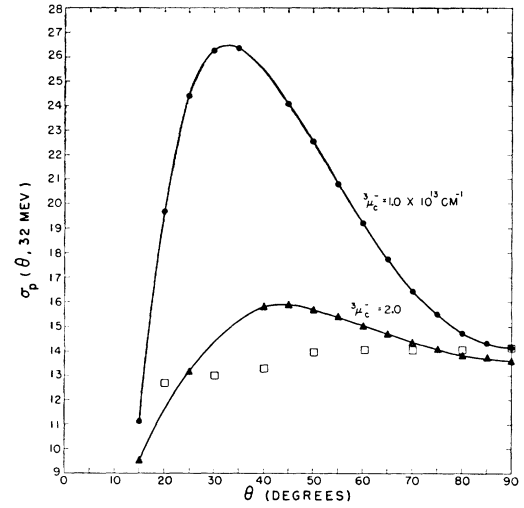

FIG. 3. $\sigma_p(\theta,32$ Mev) in mb calculated from two of the triplet odd-parity potentials of Table VI and the singlet even-parity potential of Table II whose core size is 0.5×10^{-13} cm. The open squares represent experimental data. This figure illustrates that even though a potential may predict the 32-Mev cross section at 90° correctly, it may nevertheless give a bad fit to the 32-Mev angular distribution.

Triplet odd-parity potentials which satisfy Eq. (3) for $E=32$ and 340 Mev for various $^3r_0$ and $^1r_0$ are given in Table V.

Finally, Eq. (3) must also be satisfied for $E=147$ Mev. The values of $^3\sigma_p(90°,147\text{ Mev};^3r_0)$ calculated from the potentials of Table V are also shown in Table V. Comparing these with the values of $^3\sigma_p(90°,147\text{ Mev})-{}^1\sigma_p(90°,147\text{ Mev};^1r_0)$ given in Table III, we see that Eq. (3) is satisfied only for $^1r_0=0.5\times10^{-13}$ cm.

Thus we have now determined the singlet even-parity potential. Acceptable triplet odd-parity potentials are given in Table VI.

TABLE IV. Triplet odd-parity potentials which have no central part and which satisfy Eq. (3) for $E=32$ and $E=340$ Mev.

$^1r_0$ (10^{-13} cm)	$^3r_0$ (10^{-13} cm)	$^3\mu_t^+$ (10^{13} cm^{-1})	$^3V_t^-$ (Mev)
0.1	0.1	2.0	−296
	0.2	2.0	−320
	0.4	2.13	−500
0.2	0.1	1.72	−200
	0.2	1.74	−220
	0.4	1.80	−300
0.3	0.1	1.45	−125
	0.4	1.60	−205
0.4	0.1	1.24	− 78
	0.4	1.34	− 11.5
0.5	0.1	0.98	− 40
	0.4	1.05	− 50
	0.5	1.12	− 57.5
0.6	0.1	0.65	− 10
	0.4	0.72	− 15

V. HIGH-ENERGY *n-p* TOTAL CROSS SECTIONS, THE TRIPLET SHAPE-DEPENDENT PARAMETER AND THE PERCENT *D* STATE

Let $\sigma_n(\text{total},E)$ be the *n-p* total cross section at energy E. Let $^1\sigma_n{}^+(\text{total},E;0.5\times10^{-13}\text{ cm})$ be the contribution of the singlet even parity potential (+ denotes even parity; − denotes odd parity) determined in the foregoing paragraphs to $\sigma_n(\text{total},E)$. Let $^3\sigma_n{}^+(\text{total},E;{}^3r_t{}^+/{}^3r_c{}^+,{}^3r_0)$ be the contribution of the potentials of Table I to $\sigma_n(\text{total},E)$. We must have

$$^3\sigma_n{}^+(\text{total},E;{}^3r_t{}^+/{}^3r_c,{}^3r_0) < \sigma_n(\text{total},E)-{}^1\sigma_n(\text{total},E;0.5\times10^{-13}\text{ cm}), \quad (4)$$

because odd-parity potentials also contribute to $\sigma_n(\text{total},E)$.

Values of the right-hand side of Eq. (4) are given in Table VII. Table VII also has values of the left-hand

TABLE V. Triplet odd-parity potentials which satisfy Eq. (3) for $E=32$ and $E=340$ Mev. In the last column, the left-hand side of Eq. (3) is given for $E=147$ Mev. An asterisk in the last column indicates that the 32-Mev angular distribution calculated from this potential and any of the singlet even-parity potentials in Table II is very bad. (See Fig. 3.)

${}^1r_0$ (10^{-13} cm)	${}^3r_0$ (10^{-13} cm)	${}^3\mu_t^-$ (10^{13} cm^{-1})	${}^3V_t^-$ (Mev)	${}^3\mu_c^-$ (10^{13} cm^{-1})	${}^3V_c^-$ (Mev)	${}^3\sigma_P$(90°, 147 Mev ${}^3r_0$) mb
0.2	0.4	1.9	−345	1.0	12	5.77
				2.0	100	5.95
		2.4	−727	2.0	285	6.30
0.4	0.4	2.0	−318	0.6	30	···
				1.0	100	*
				1.5	285	···
				2.0	670	4.95*
		1.6	−173.5	1.5	180	5.46
				2.0	400	5.57
		1.4	−120	2.0	250	5.24
0.5	0.4	1.2	− 63	1.5	205	3.82
				2.0	570	4.19
		1.1	− 50.4	0.6	14.8	3.27
				1.0	47.0	3.39
				1.5	150	3.57
				2.0	400	3.75
				3.0	2000	···
	0.5	1.1	− 52.5	3.0	3000	···
		1.12	− 57.5	1.5	150	3.44
		1.16	− 62.5	1.5	200	···

side of Eq. (4) calculated from the potentials of Table I.

Figure 4 is prepared (in part) from Table VII. The line marked 40 Mev (for example) is determined in the following way. Each potential in Table I is characterized by two parameters ${}^3r_0$ and ${}^3r_t^+/{}^3r_c^+$ and so corresponds to a point in Fig. 4 whose coordinates are ${}^3r_0$ and ${}^3r_t^+/{}^3r_c^+$. If this point lies above the line marked $E=40$ Mev, this potential satisfies Eq. (4) for $E=40$ Mev. For $E=156$ Mev, the acceptable region is above and to the right of the curve.

TABLE VI. Triplet odd-parity potentials which satisfy Eq. (3) for $E=32$, 147, and 340 Mev. It is possible to satisfy Eq. (3) only for ${}^1r_0=0.5\times10^{-13}$ cm. The last column contains values of σ_n(0,90 Mev) calculated by combining these triplet odd-parity potentials with the singlet even-parity potential whose core is 0.5×10^{-13} cm and triplet even-parity potentials number 7 from Table I for ${}^3r_0=0.4\times10^{-13}$ cm, and number 8 for ${}^3r_0=0.5\times10^{-13}$ cm. σ_n(0,90 Mev) is not sensitive to the singlet odd-parity potential

${}^3r_0$ (10^{-13} cm)	${}^3\mu_t^-$ (10^{13} cm^{-1})	${}^3V_t^-$ (Mev)	${}^3\mu_c^-$ (10^{13} cm^{-1})	${}^3V_c^-$ (Mev)	σ_n(0, 90 Mev) (mb)
0.4	1.1	−50.4	1.0	47	17
			1.5	150	16
			2.0	400	15.2
			3.0	2000	14.8
	1.06	−47	1.5	100	13.8
	1.02	−44	1.5	40	11.8
	0.96	−37	···	0	10.6
0.5	1.16	−62.5	1.5	200	15.2
	1.12	−57.5	1.5	150	13.3
	1.02	−47.2	···	0	9.2

TABLE VII. Values of ${}^3\sigma_n^+$(total,E) for the potentials of Table I compared to σ_n(total,E)$-{}^1\sigma_n$(total,E;0.5×10^{-13} cm). See Eq. (4).

E (Mev)	19.66	28	40	90	156	280
σ_n(total,E) (mb)	484	315	220	80	49	36
${}^1\sigma_n$(total,E; 0.5×10^{-13} cm) (mb)	79.8	47.5	26.3	4.94	3.03	5.05
Difference (mb)	404.2	267.5	193.7	75.05	45.97	30.95
Identification No.			${}^3\sigma_n^+$(total,E) in mb			
14	···	295.1	215.5	85.2	45.3	···
11	408.5	286.3	196.2	78.1	41.0	20.8
3	403.2	279.1	187.5	72.0	38.7	22.2
6	399.7	273.0	179.8	66.6	38.3	26.8
13	405.6	285.7	197.3	83.8	47.0	25.0
10	401.8	278.5	189.6	76.8	43.5	···
2	399.4	273.2	181.1	70.6	41.7	26.6
5	397.5	269.3	175.2	66.1	42.8	32.7
12	401.3	279.8	191.8	82.9	49.5	···
9	399.4	···	···	76.3	46.6	29.7
1	398.3	272.4	179.8	71.4	46.1	···
4	397.0	268.8	174.5	67.3	47.3	···

An analysis[15] of the low-energy n-p and p-p data shows that the triplet shape-dependent parameter (${}^3P$ defined by Blatt and Jackson) cannot be positive. The

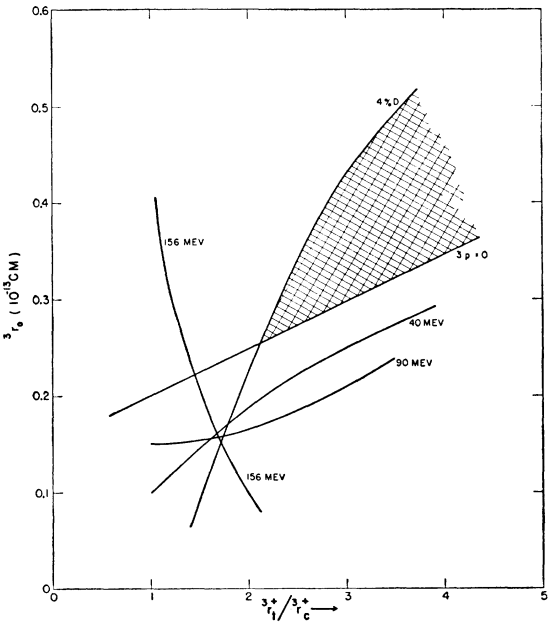

FIG. 4. Limitations on the triplet even-parity potentials of Table I. The cross-hatched region represents the most acceptable potentials. Most of the potentials of Table I fall outside this region. Potentials lying above the curve marked ${}^3P=0$ have negative shape-dependent parameters as required by the low-energy data. Potentials lying below the curve marked 4% D give less than 4% D state for the deuteron. Potentials lying above the curve marked 40 Mev (for example) satisfy Eq. (4) for $E=40$ Mev.

[15] This analysis was done in the following way. The contribution of the singlet even-parity potential with ${}^1r_0=0.5\times10^{-13}$ cm, the least contribution of any of the triplet odd-parity potentials in Table VI, and the least contribution of the states for $l\geq2$ calculated from the triplet even parity potentials of Table I to σ_n(total,E) were subtracted from experimental values of σ_n(total,E) in the energy range $E<20$ Mev. The difference was taken to be

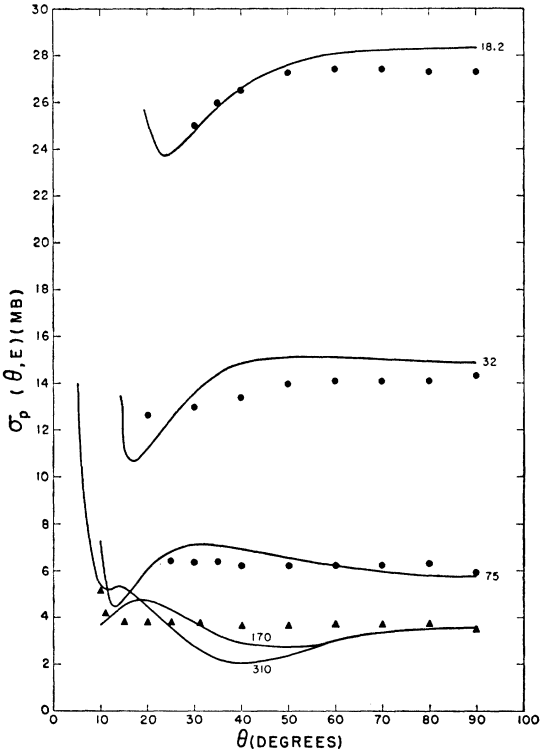

FIG. 5. Final fit to the p-p angular distributions for a number of energies.

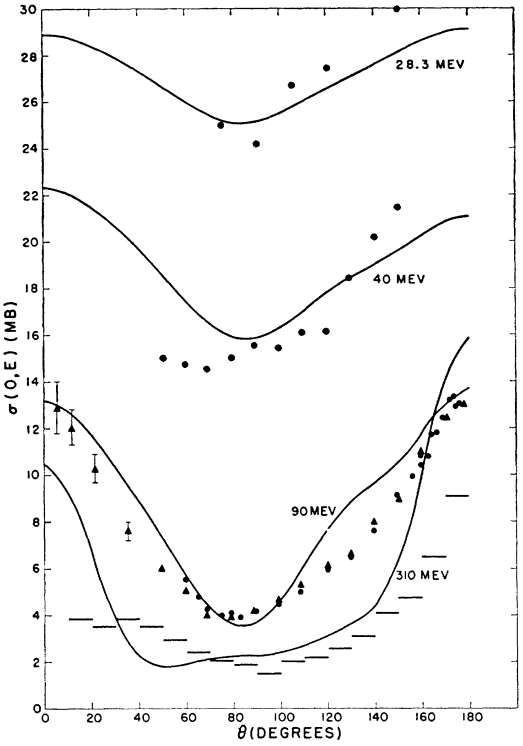

FIG. 6. Final fit to the n-p angular distributions for a number of energies.

acceptable region is above the curve marked ${}^3P=0$ in Fig. 4. This curve may be thought of as the low-energy limit of the family of curves marked 156, 90, and 40 Mev.

If we accept four percent as an upper limit for the percent D state, the acceptable region is below the curve marked 4% D.

The different definitions of the boundaries of the acceptable region agree very well and limit the acceptable triplet even-parity potentials to the region roughly described by ${}^3r_0 \geq 0.3\times10^{-13}$ cm and ${}^3r_t{}^+/{}^3r_c{}^+ > 3.0$ and described more accurately by Fig. 4. Acceptable triplet even-parity potentials are given in Table VIII.

TABLE VIII. Triplet even-parity potentials which fall in the acceptable region in Fig. 4.

Identification number	${}^3r_0$ (10^{-13} cm)	${}^3r_t{}^+/{}^3r_c{}^+$	${}^3V_c{}^+$ (Mev)	${}^3r_c{}^+$ (10^{-13} cm)	${}^3V_t{}^+$ (Mev)	${}^3r_t{}^+$ (10^{-13} cm)
3	0.3	2.857	595.7	0.5714	26.00	1.633
6	0.4	2.857	1308	0.4762	44.79	1.361
7	0.4	4.0	2640	0.3921	30.00	1.568
8	0.5	4.0	6395	0.3405	45.00	1.362

the ${}^3S_1$ contribution to σ_n(total,E). This ${}^3S_1$ contribution was analyzed in terms of an effective-range expansion assuming that the triplet scattering length is 5.38×10^{-13} cm. The resulting ${}^3P$ was negative. Omitting the estimated triplet contributions for $l\neq0$ requires an even more negative ${}^3P$.

VI. n-p ANGULAR DISTRIBUTION AT $E=90$ Mev

We take a triplet even-parity potential from Table VIII and combine it with one of the triplet odd-parity potentials of Table VI (the assumption, made at the outset, that the triplet even-parity potential and the triplet odd-parity potential have the same core size now serves to limit the possible number of combinations) and the singlet even-parity potential decided on at the end of Sec. IV. With these potentials and ${}^1V_c{}^-=0$, we calculate $\sigma_n(\theta,90$ Mev).

We see that $\sigma_n(180°;90$ Mev) is not nearly large enough. This means that we are going to have to take ${}^1V_c{}^-$ negative. [A sufficiently positive ${}^1V_c{}^-$ would also increase $\sigma_n(180°,90$ Mev), but it would also increase $\sigma_n(0°,90$ Mev) and σ_n(total,E) in a way which would make it difficult to fit experimental data.] Meson theory calculations[6] also suggest a repulsive ${}^1V_c{}^-$. Experience shows this additional singlet odd-parity potential will not change $\sigma_n(0°,90$ Mev) by more than

TABLE IX. Triplet odd-parity potentials which give the experimental value of $\sigma_n(0,90$ Mev) when combined with the singlet even-parity potential whose core size is 0.5×10^{-13} cm, and triplet even-parity potential number 7 of Table VIII for ${}^3r_0=0.4\times10^{-13}$ cm and number 8 for ${}^3r_0=0.5\times10^{-13}$ cm.

${}^3r_0$ (10^{-13} cm)	${}^3\mu_t{}^-$ (10^{13} cm^{-1})	${}^3V_t{}^-$ (Mev)	${}^3\mu_c{}^-$ (10^{13} cm^{-1})	${}^3V_c{}^-$ (Mev)
0.4	1.06	−47	1.5	100
0.5	1.12	−57.5	1.5	150

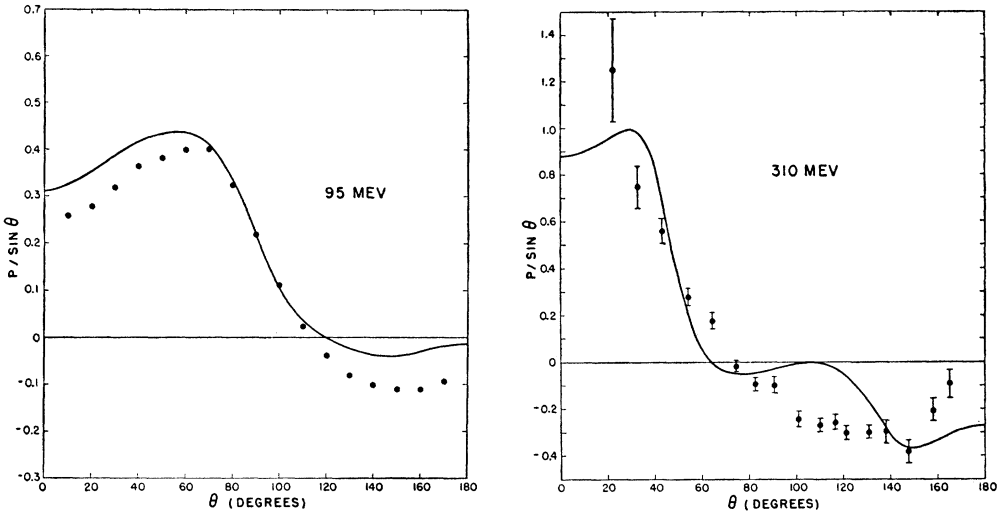

FIG. 7. Final fit to the n-p polarizations for $E=95$ and $E=310$ Mev.

0.2 mb; 0.2 mb is within the accuracy to which $\sigma_n(0°,90\text{ Mev})$ is known, and is zero for our purposes.

For fixed even-parity potentials, $\sigma_n(0°,90\text{ Mev})$ depends mostly on ${}^3\mu_t^-$. This is illustrated in Table VI for the triplet even parity potentials number 7 and 8 of Table I. Fitting the experimental value of $\sigma_n(0°,90\text{ Mev})$ (13.5 mb) determines ${}^3\mu_t^-$ and so eliminates some of the triplet odd-parity potentials of Table VI. Remaining acceptable triplet odd-parity potentials are given in Table IX.

Fitting the experimental value of $\sigma_n(180°,90\text{ Mev})$ (13.5 mb) determines ${}^1V_c^-$ as a function of ${}^1\mu_c^-$. [Because we have assumed that the singlet even- and odd-parity potentials have the same core size, we must take ${}^1r_0=0.5\times10^{-13}$ cm in fitting $\sigma_n(180°,90\text{ Mev})$.] The function depends on what ${}^3r_0$ is used. Sample acceptable singlet odd-parity potentials are given in Table X for ${}^3r_0=0.5\times10^{-13}$ cm.

VII. n-p ANGULAR DISTRIBUTIONS AT LOW ENERGIES

The experimental value (1.09)[16] of the ratio $\sigma_n(180°,E)/\sigma_n(90°,E)$ at $E=19.66$ Mev then determines ${}^1\mu_c^-$. The values of $\sigma_n(180°,E)/\sigma_n(90°,E)$ calculated with the potentials of Table X are compared with experimental value in Table X. The range of the odd-parity singlet potential must be long, but is not very well determined.

TABLE X. Singlet odd-parity potentials which give correctly the experimental value of $\sigma_n(180°,90\text{ Mev})$ when combined with the singlet even parity potential whose core size is ${}^1r_0=0.5\times10^{-13}$ cm, the triplet even parity potential number 8 from Table VIII, and the triplet odd parity potential in Table IX whose core size is 0.5×10^{-13} cm. In the last columns, the values of $\sigma_n(180°,19.66\text{ Mev})/\sigma_n(90°,19.66\text{ Mev})$ calculated with these potentials are compared with the experimental value 1.09.[a]

${}^1r_0$ (10^{-13} cm)	${}^1\mu_c^-$ (10^{13} cm^{-1})	${}^1V_c^-$ (Mev)	$\sigma_n(180°,19.66\text{ Mev})/\sigma_n(90°,19.66\text{ Mev})$ calc	exptl.
0.5	0.6	− 23.2	1.15	1.09
	1.0	−113.0	1.096	

[a] See reference 16.

[16] J. E. Perry, Jr., Los Alamos Scientific Laboratory (private communication).

VIII. FINAL FIT TO THE DATA

The potential thus determined which appears to give the best over-all fit to all the data is characterized by the following parameters:

$$\begin{aligned}
&{}^3r_0={}^1r_0=0.5000\times10^{-13}\text{ cm},\\
&{}^1V_c^+=\begin{cases}914.6\text{ Mev for }n\text{-}p\\ 896.6\text{ Mev for }p\text{-}p,\end{cases}\\
&{}^1r_c^+=0.5880\times10^{-13}\text{ cm},\\
&{}^3V_c^{(-)}=+150.0\text{ Mev},\\
&{}^3r_c^{(-)}=0.6667\times10^{-13}\text{ cm},\\
&{}^3V_t^{(-)}=-57.50\text{ Mev},\\
&{}^3r_t^{(-)}=0.8930\times10^{-13}\text{ cm},\\
&{}^1V_c^{(-)}=-113.0\text{ Mev},\\
&{}^1r_c^{(-)}=1.000\times10^{-13}\text{ cm},\\
&{}^3V_c^{(+)}=6395\text{ Mev},\\
&{}^3r_c^{(+)}=0.3405\times10^{-13}\text{ cm},\\
&{}^3V_t^{(+)}=45.00\text{ Mev},\\
&{}^3r_t^{(+)}=1.362\times10^{-13}\text{ cm}.
\end{aligned}\tag{5}$$

This potential gives 4.19% for the percent D state.

In Figs. 5–8 are illustrated the n-p and p-p angular distributions and polarizations calculated from this potential. The phase shifts calculated from this potential are given in Tables XI through XIII. It is seen that reasonably good fits are obtained to the proton scattering data, except at the highest energy (340 Mev). Likewise, the neutron-proton scattering data appears

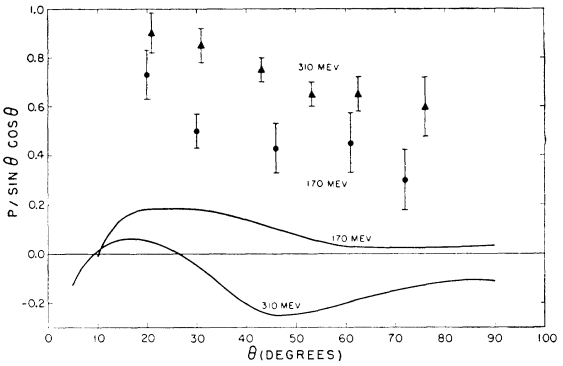

FIG. 8. Final fit to the p-p polarization for $E=310$ and $E=170$ Mev.

to fit the data rather well except at high energies. It is seen that at 90 Mev the calculated n-p angular distribution is more "V"-shaped than the data indicate. Generally, the fit obtained may be said to reproduce the data accurately at low energies and qualitatively at high energies.

The calculated n-p polarizations agree with the experimental n-p polarization even at the highest energies. This gives weight to the view that potentials of the form we have used correctly describe the triplet even-parity interaction even at high energies.

There is a qualitative discrepancy between the calculated and experimental values of the high-energy p-p polarization data. Potentials of the sort discussed above give the opposite sign of the polarization than that determined experimentally. This difficulty casts doubt upon the qualitative correctness of the triplet odd-parity potentials.

TABLE XI. Singlet phase shifts. These are twice the Blatt-Biedenharn phase shifts as used by Stapp *et al.*, in radians.

E (Mev)	$^1S_0$	$^1P_1$	$^1D_2$	$^1F_3$	$^1G_4$	$^1H_5$
10	2.038	−0.0881	0.00225	···	···	···
20	1.768	−0.1796	0.0114	···	···	···
30	1.552	−0.2550	0.0259	···	···	···
40	1.373	−0.3178	0.0460	−0.0176	···	···
50	1.217	−0.3715	0.0693	−0.0256	···	···
60	1.079	−0.4165	0.0945	−0.0340	···	···
70	0.9586	−0.4566	0.1230	−0.0439	···	···
80	0.8432	−0.4935	0.1526	−0.0532	···	···
90	0.7381	−0.5255	0.1812	−0.0609	···	···
100	0.6411	−0.5536	0.2106	−0.0693	···	−0.0102
120	0.4678	−0.6072	0.2722	−0.0878	0.0136	−0.0146
140	0.3087	−0.6522	0.3271	−0.1008	0.0172	−0.0179
160	0.1674	−0.6919	0.3833	−0.1167	0.0261	−0.0252
180	0.0383	−0.7323	0.4333	−0.1304	0.0321	−0.0278
200	−0.0861	−0.7646	0.4768	−0.1396	0.0381	−0.0322
220	−0.1982	−0.7970	0.5220	−0.1537	0.0497	−0.0401
240	−0.3019	−0.8321	0.5587	−0.1651	0.0570	−0.0426
260	−0.4058	−0.8603	0.5887	−0.1709	0.0627	−0.0450
280	−0.5033	−0.8865	0.6214	−0.1812	0.0748	−0.0532
300	−0.5905	−0.9186	0.6495	−0.1935	0.0860	−0.0585

The singlet even-parity potential for $^1r_0=0.4\times10^{-13}$ cm gives correctly the $^1S_0$, $^1D_2$, and $^1G_4$ phase shifts which Stapp *et al.*[17] found for the first and third solutions to their analysis of the 310-Mev p-p data. Thus it seems that potentials of the form we have used correctly describe the singlet even-parity interaction, even at high energies.

The triplet P phase shifts shown in Table XII for $E=300$ Mev are not remotely similar to the triplet P phase shifts of any of the first four solutions of Stapp *et al.*[17] For all energies, the triplet P phase shifts shown in Table XII are not similar to the Feshbach-Lomon[18] triplet P phase shifts. Finally, Phillips[19] in a phase shift analysis of the 95-Mev n-p and p-p data found even-parity phase shifts quite similar to those shown in Tables XI and XIII for $E=90$ Mev, but triplet P

TABLE XII. Triplet odd-parity phase shifts. These are twice the Blatt-Biedenharn phase shifts as used by Stapp *et al.*, in radians.

E (Mev)	$^3P_0$	$^3P_1$	$^3P_2$	$^3F_2$	$2\epsilon(2)$	$^3F_3$	$^3F_4$	$^3H_4$	$2\epsilon(4)$	$^3H_5$	$^3H_6$
10	0.2096	−0.0411	0.0367	···	0.2470	···	···				
20	0.4785	−0.0856	0.0860	···	0.3889	···	···				
30	0.7047	−0.1225	0.1331	···	0.4687	···	···				
40	0.8716	−0.1537	0.1743	···	0.5398	···	···				
50	0.9899	−0.1807	0.2089	···	0.5946	−0.0110	···				
60	1.071	−0.2030	0.2385	···	0.6420	−0.0145	0.0142				
70	1.124	−0.2241	0.2612	···	0.6864	−0.0194	0.0184				
80	1.158	−0.2441	0.2793	···	0.7317	−0.0236	0.0240				
90	1.180	−0.2613	0.2947	···	0.7731	−0.0264	0.0306				
100	1.189	−0.2768	0.3063	···	0.8129	−0.0300	0.0366				
120	1.186	−0.3100	0.3179	···	0.8983	−0.0390	0.0473				
140	1.169	−0.3382	0.3258	···	0.9878	−0.0431	0.0617				
160	1.136	−0.3665	0.3242	···	1.080	−0.0508	0.0719	···	0.9176	−0.0118	0.0103
180	1.100	−0.3969	0.3205	−0.0106	1.184	−0.0563	0.0844	···	0.9452	−0.0118	0.0157
200	1.061	−0.4214	0.3179	−0.0139	1.288	−0.0582	0.0981	···	0.9292	−0.0135	0.0186
220	1.014	−0.4494	0.3085	−0.0251	1.395	−0.0654	0.1061	···	0.9345	−0.0187	0.0198
240	0.9702	−0.4800	0.3020	−0.0373	1.511	−0.0699	0.1174	···	0.9563	−0.0185	0.0260
260	0.9271	−0.5043	0.2998	−0.0471	1.619	−0.0694	0.1309	···	0.9453	−0.0184	0.0304
280	0.8773	−0.5299	0.2924	−0.0640	1.721	−0.0742	0.1379	···	0.9379	−0.0240	0.0307
300	0.8290	−0.5615	0.2851	−0.0863	1.824	−0.0807	0.1447	···	0.9554	−0.0268	0.0347

[17] Stapp, Ypsilantis, and Metropolis, preceding paper [Phys. Rev. **105**, 302 (1957)].
[18] H. Feshbach and F. Lomon, Phys. Rev. **102**, 891 (1956).
[19] R. J. N. Phillips, Atomic Energy Research Establishment, Harwell, Berkshire, England (unpublished).

TABLE XIII. Triplet even-parity phase shifts. These are twice the Blatt-Biedenharn phase shifts as used by Stapp *et al.*, in radians.

E (Mev)	$^3S_1$	$^3D_1$	$2\epsilon(1)$	$^3D_2$	$^3D_3$	$^3G_3$	$2\epsilon(3)$	$^3G_4$	$^3G_5$
10	3.578	−0.0424	...	0.0400	...	...	0.6710	...	...
20	2.996	−0.1162	0.0095	0.1208	−0.0374	0.0131	1.219	...	...
30	2.637	−0.1875	0.0275	0.2061	−0.0642	0.0256	1.344	0.0131	...
40	2.373	−0.2498	0.0424	0.2886	−0.0894	0.0408	1.452	0.0240	−0.0142
50	2.160	−0.3038	0.0545	0.3651	−0.1137	0.0568	1.544	0.0353	−0.0224
60	1.981	−0.3515	0.0636	0.4364	−0.1343	0.0722	1.616	0.0480	−0.0308
70	1.826	−0.3916	0.0704	0.5051	−0.1508	0.0881	1.687	0.0616	−0.0384
80	1.686	−0.4256	0.0752	0.5695	−0.1651	0.1031	1.757	0.0739	−0.0473
90	1.560	−0.4564	0.0782	0.6297	−0.1782	0.1167	1.820	0.0856	−0.0571
100	1.446	−0.4835	0.0797	0.6886	−0.1891	0.1318	1.876	0.0983	−0.0645
120	1.242	−0.5232	0.0786	0.8013	−0.2039	0.1640	1.993	0.1227	−0.0800
140	1.060	−0.5544	0.0724	0.9025	−0.2180	0.1935	2.098	0.1425	−0.0961
160	0.9009	−0.5754	0.0617	1.001	−0.2251	0.2289	2.192	0.1655	−0.1078
180	0.7542	−0.5862	0.0461	1.088	−0.2320	0.2637	2.284	0.1831	−0.1212
200	0.6176	−0.5966	0.0252	1.169	−0.2398	0.2971	2.362	0.1998	−0.1326
220	0.4966	−0.5983	−0.0020	1.247	−0.2408	0.3369	2.434	0.2203	...
240	0.3821	−0.5939	−0.0369	1.311	−0.2439	0.3735	2.501	0.2348	...
260	0.2707	−0.5930	−0.0818	1.370	−0.2502	0.4065	2.558	0.2477	...
280	0.1713	−0.5885	−0.1399	1.428	−0.2503	0.4452	2.608	0.2662	...
300	0.0821	−0.5775	−0.2157	1.473	−0.2486	0.4828	2.656	0.2820	...

phase shifts similar to those of Feshbach and Lomon. Wolfenstein[20] concluded from his study of the 310-Mev p-p data that if Born's approximation is valid for the triplet odd-parity interaction, then it must contain a strong spin-orbit term. It seems certain, therefore, that the triplet odd-parity interaction cannot be understood in terms of the simple potentials we have used.

[20] L. Wolfenstein, Bull. Am. Phys. Soc. Ser. II, 1, 36 (1956).